Electronic Supplementary Material (ESI) for Nanoscale Horizons.

Supporting Information

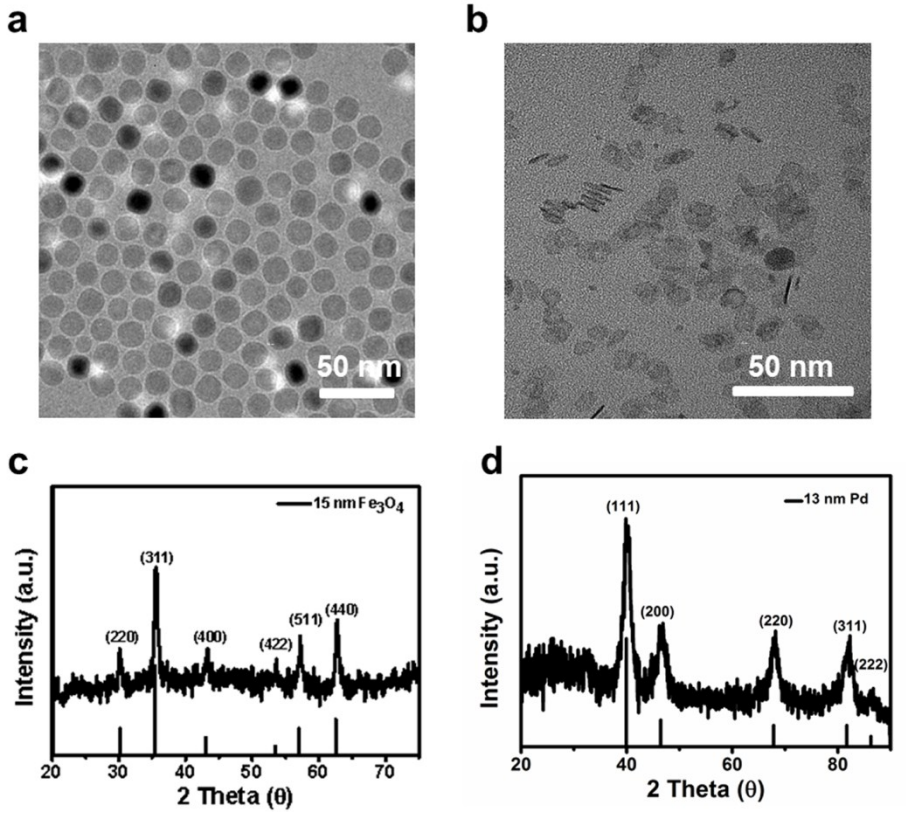

Fig. S1 TEM images of (a) Fe_3O_4 NPs and (b) Pd NSs. XRD patterns of (c) Fe_3O_4 NPs and (d) Pd NSs.

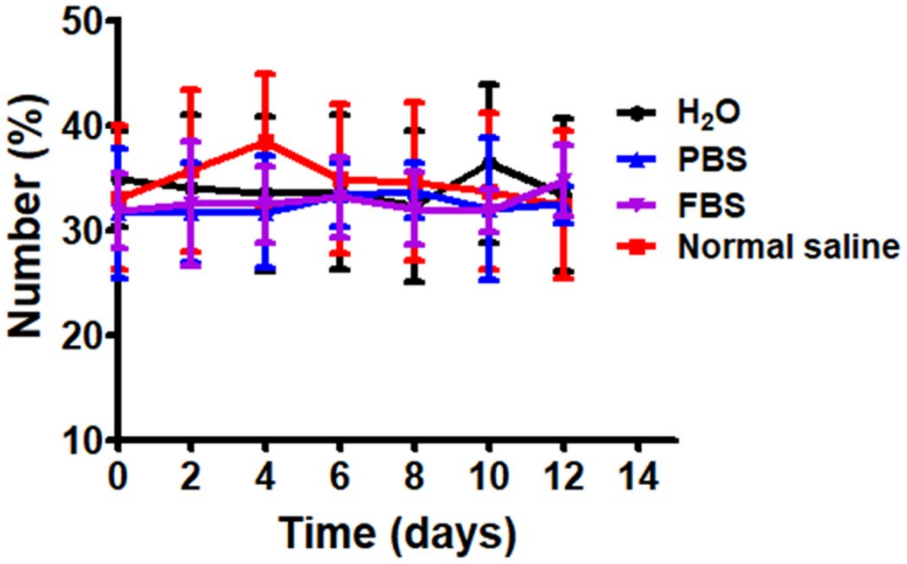

Fig. S2 Hydrodynamic size variation of Fe_3O_4-Pd JNPs as a function of time upon incubation in DI water, 10% FBS, PBS, and normal saline.

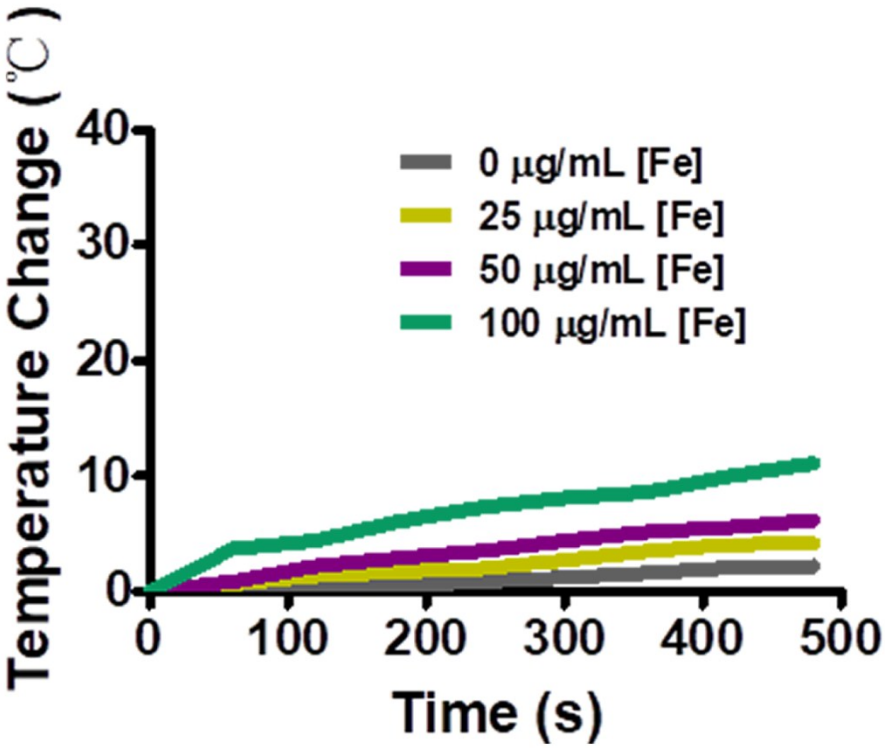

Fig. S3 Time dependent heating profiles of Fe_3O_4 NPs at various concentrations under AMF plus 808 nm laser irradiation.

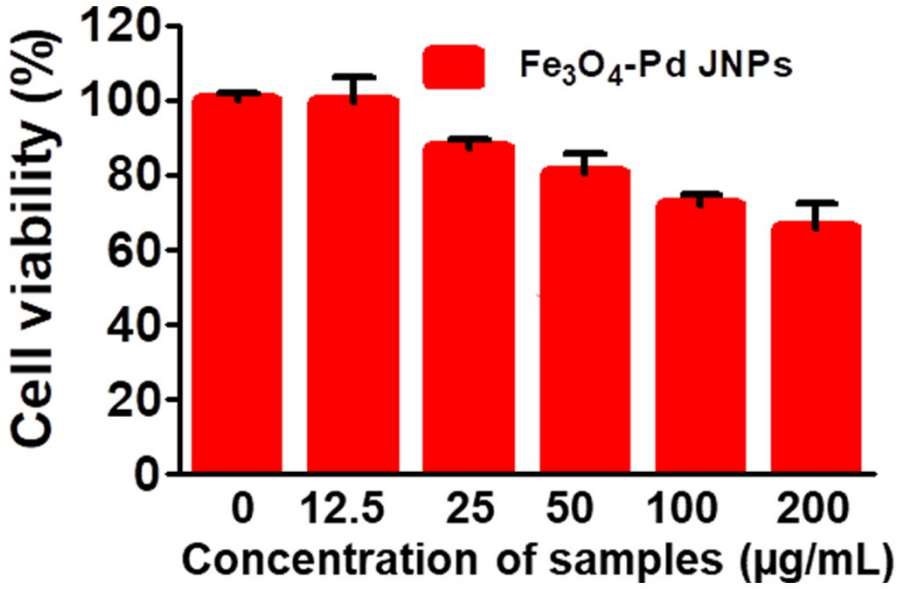

Fig. S4 Cytotoxicity evaluation of Fe_3O_4-Pd JNPs.

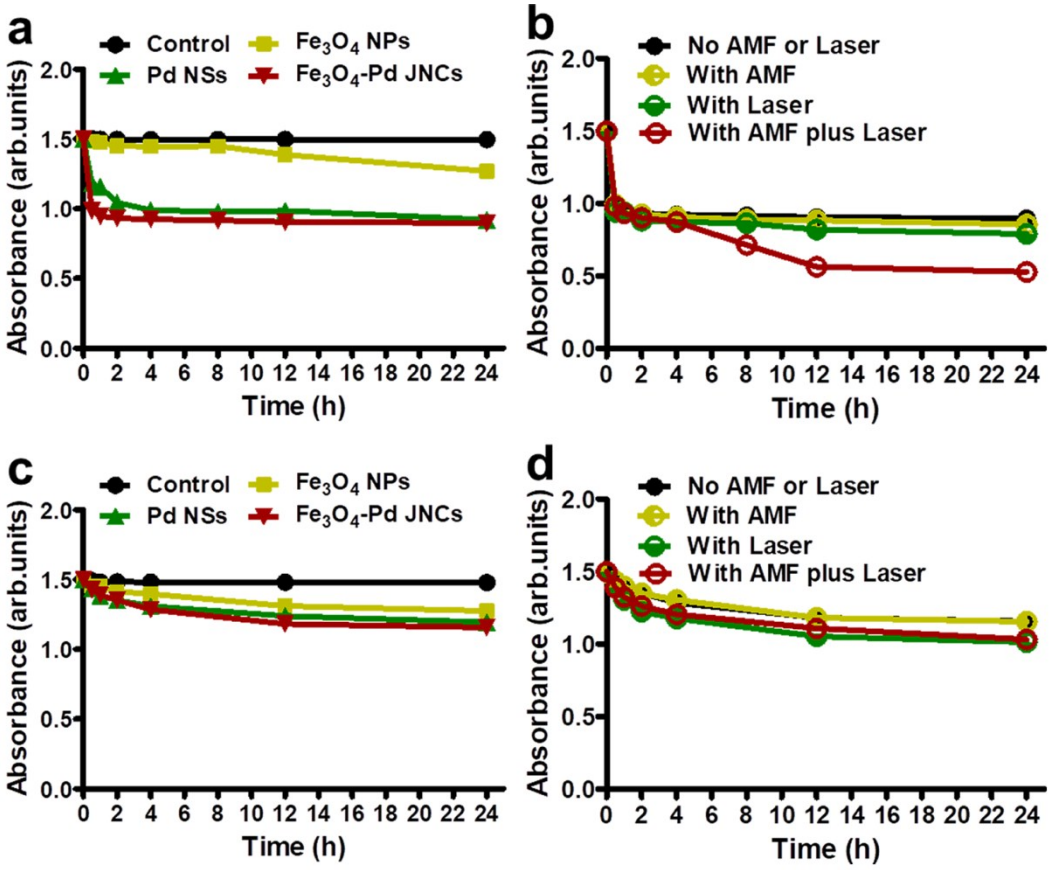

Fig. S5 a) Decay curves of MB absorption at 664 nm in different solutions as a function of time at pH 6.5. b) Decay curves of MB absorption at 664 nm for Fe_3O_4-Pd JNPs under AMF or laser or both for 8 min, as a function of time, at pH 6.5. c) Decay curves of MB absorption at 664 nm in different solutions as a function of time at pH 7.4. d) Decay curves of MB absorption at 664 nm for Fe_3O_4-Pd JNPs under AMF or laser or both for 8 min, as a function of time, at pH 7.4.

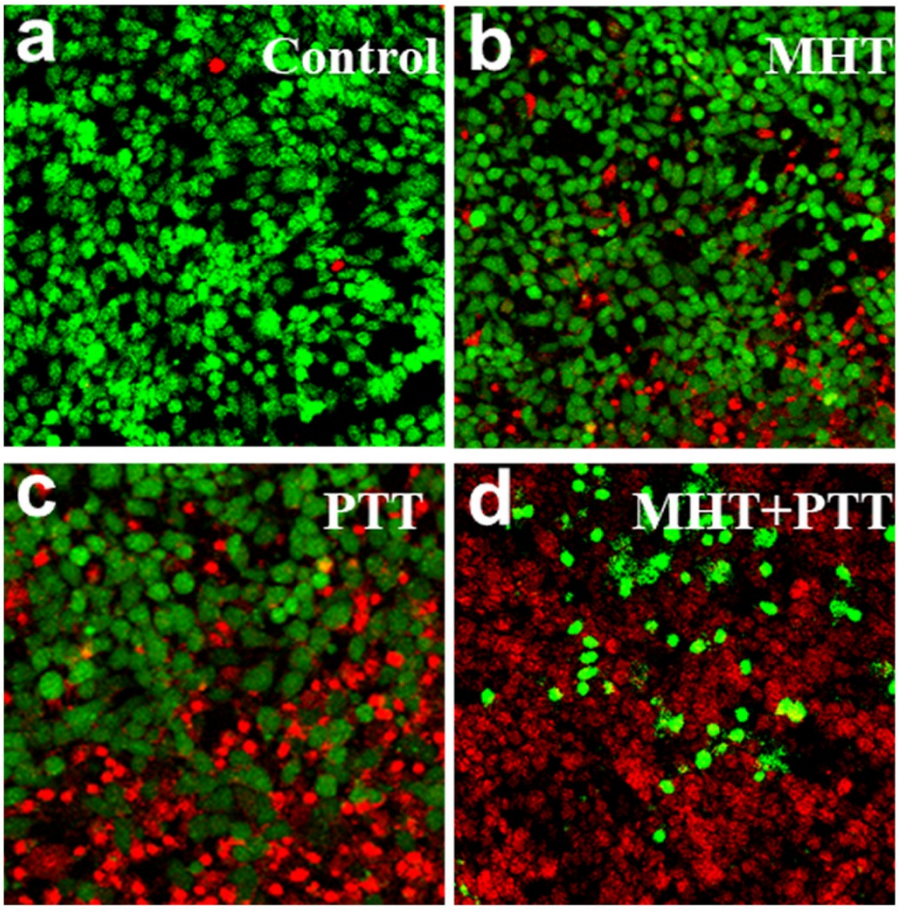

Fig. S6 Confocal images of 4T1 cells after different treatment. The cells were stained with acridine orange/ethidium bromide for 1 min. Live and dead cells appear green and orange, respectively.

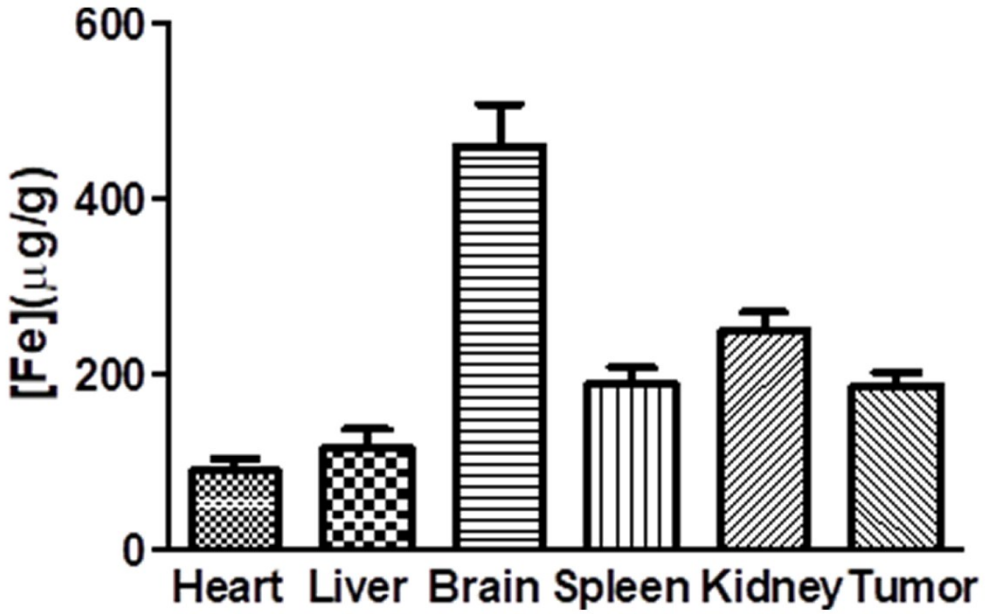

Fig. S7 Biodistribution and tumor uptake of Fe_3O_4-Pd JNPs in 4T1 tumor-bearing mice. Data are expressed as means ± s.d. (n = 3).

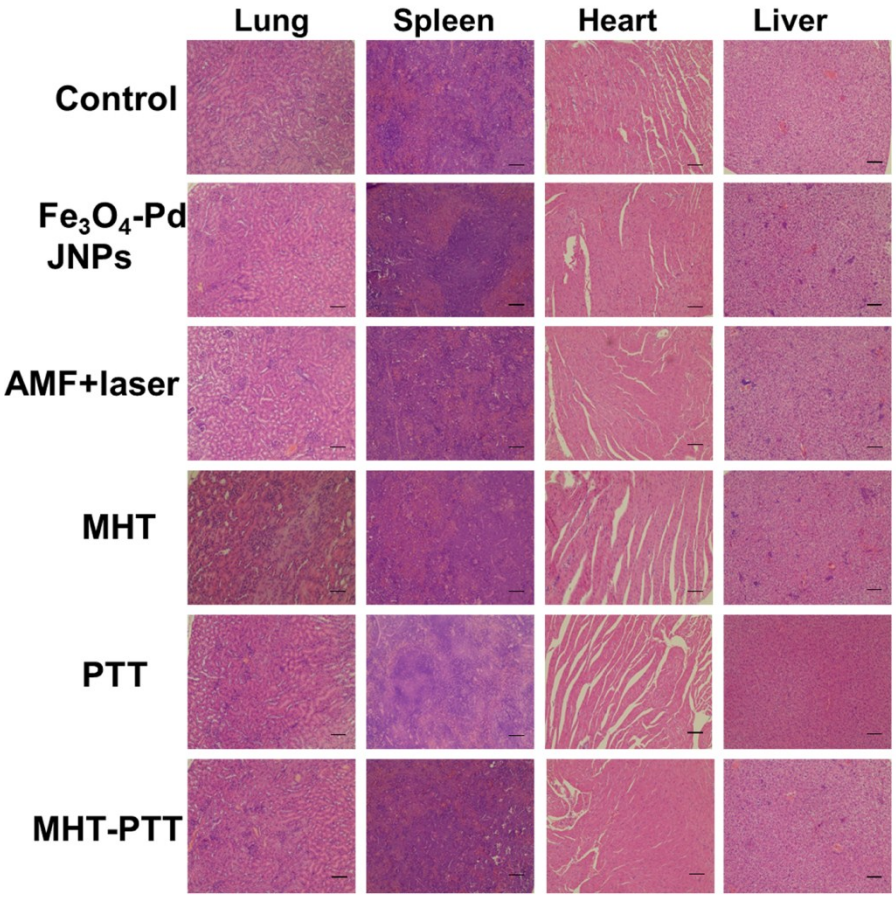

Fig. S8 H&E staining of mice organs collected from different groups.

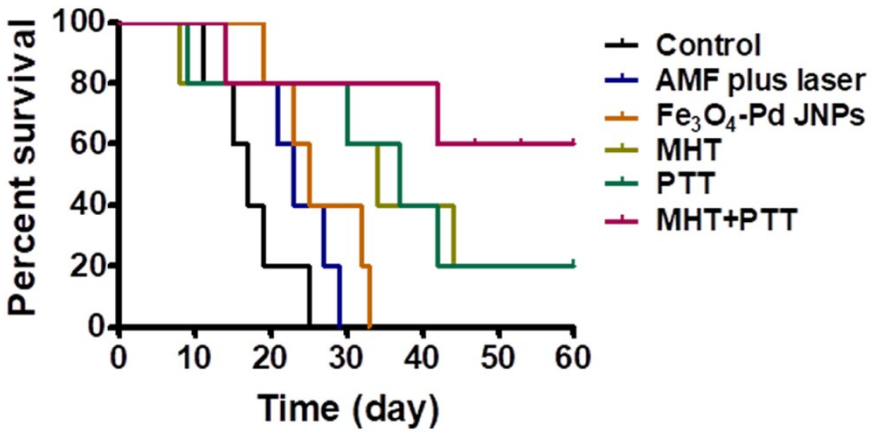

Fig. S9 Survival rate of mouse of different groups after various treatments.